Pakistan Academy of Sciences

Research Article

Flow Control in a Rectangular Open Channel using Two Impermeable Spur Dikes: A Numerical Study

Hafiz Syed Moazzum Gillani[1], Zain-ul-Hassan[1], Hafiz Rana Azeem Sarwar[2], Muhammad Sohail Jameel[1*], Waqar Hasan[1], Ehsaan Manzoor[1], and Imran Khan[1]

[1]Department of Transportation Engineering and Management, University of Engineering and Technology, Lahore, Pakistan
[2]Department of Civil Engineering, Islamic International University, Islamabad, Pakistan

Abstract: The present study examines how adjusting vegetation patches in a rectangular open channel with two impermeable spur dikes alters the displacement of the recirculation region. The Reynolds stress turbulence model is implemented via the 3D numerical code FLUENT (ANSYS). Mean stream-wise velocity profiles were drawn at selected positions and at mid of flow depth i.e., 3.5 cm, a horizontal plane is cut through the open channel for analyzing velocity contours and streamline flow. The findings indicate that the stream-wise velocity profiles showed fluctuations in the presence of different shapes and arrangement of cylindrical patch discussed and the maximum velocity within the field of spur dike is of the order of 0.018 m/s due to the prism shape. By changing the position of the cylindrical patch, the location of the recirculation region displaces within the field of impermeable spur dike.

Keywords: Recirculation Region, Vegetation Patches, Impermeable Spur Dikes, Rectangular Open Channel, Flow Control in Open Channels.

1. INTRODUCTION

The essential sources of water are rivers as well as channels for a long period. To make water accessible, the human beings used to live near rivers and channels which served the purpose of transferring water to far areas. The previous reason makes it essential to protect the channels and rivers from erosion as well as their deterioration due to flowing water. Researchers from diverse scientific disciplines such as Hydraulics, Hydrology, Geology, and Sedimentology have collectively worked to demonstrate that comprehensively analyzing river channels and their historical behaviors, along with foundational scientific and technical investigations, is distinctly separate when aiming to optimize the utilization of these crucial water resources. Spur dikes are the hydraulic structures used for river training and bank protection works. The use of spur dikes from long ago shows that this kind of structure has wide benefits. By constructing the spur dike, the flow path contracts, and resultantly

the flow velocity near the structure increases which leads to increased average velocity in the contracted section. This is why using spur dikes is a good solution for managing how rivers flow, controlling the movement of water and passage of water under bridges, and preventing the erosion of river banks and edges [1].

Spur dikes are commonly used in channels to prevent the erosion of channel beds and banks by fixing them at the right angle to the direction of flow in order to reduce the velocity of flow. These are considered among the best structures of hydro engineering for prevention and diversion of water. The Spur Dikes are of two types: Pervious Spur Dikes and Impervious Spur Dikes, based on the fact that the structure is pervious or not. Generally, construction material used for spur dikes are bamboo, steel, timber, RCC piles etc. Permeable Spur dikes are considered economical and found their application in temporary works. Construction materials for impervious spur dikes are stones, soils

(local), gravels, rocks, and local materials (easily available). An approaching flow is prevented or diverted through impervious spur dikes. Although water can pass through pervious spur dike, but it reduces the water speed. Either the spur dikes are covered by water or not, these are classified as submerged and non-submerged type. If the spur dike is covered by water, then this is referred as submerged spur dike. If the spur dike is not fully covered by water, it is known as non-submerged spur dikes. Based on the shape, spur dikes may have shape like hocky shape, T-shape, mole-head as well as L-shape. Again based on function of spur dikes against water, the dikes are classified as diverting type, repelling type and attracting type. A downstream-facing (Attractive) spur dike exerts an attractive force, causing the flow to be diverted from its original path. In this way, it makes the flow of water towards the center of channel. A deflection spur dike is strategically positioned with its upstream end facing the flow of the river. Its purpose is to redirect the water away from the riverbank in order to mitigate erosion by redirecting the water flow. Consequently, the repelling spur dike is anchored perpendicular to the flow's direction [2].

Variations in the water bodies (i.e., river) beds and banks results due to different features such as shape of channel (width, depth), the material from which river bed is made-up, amount of sediment carried by water bodies. In the past, researchers simulated actual flow conditions in open channels with different flow conditions so that properties of flow under different conditions can be determined. In this regard, Koken *et al*. [3] employed an impermeable spur dike within a horizontal plane, utilizing two-dimensional velocity vectors, to examine flow mechanisms downstream. Exploring flow patterns around both individual and arrays of water-resistant spur dikes, Kafle *et al*. [4] employed different turbulent closure models. Teraguchi *et al.* [5] analyzed the impact on flow velocity distribution around pervious and impervious spur dikes, as well as bandal-like structures, under two conditions: one where these were non-submerged, and the other where the submerged state prevailed. At downstream, the vortex zone formed around one impervious spur dike was investigated using RNG (Re-Normalization Group model) turbulence method by Giglou *et. al* [1]. When water passed

through impervious spur dike, it resulted into vortex zone formed around impervious spur dike of four times the length of spur dike. This caused decrease in flow velocity of silt which caused deposition of silt. With passage of time, due to silt deposition the spur dike field would be filled with silt. This becomes the reason of reduction in flood carrying capacity of rivers. RSM (Reynold's Stress Model) was used by many researchers in the past to study the velocity flow characteristics in open channels [6-8]. Around two impervious spur dikes, the distribution of momentum as well as mass horizontally and vertically was done by using LES model (Large Eddy Simulation) [9]. Vaghefi *et al.* [10] used computational fluid dynamic (CFD) model to simulate that how water flows around a T-shaped barrier in a river bend, while considering nearby structures that either attract or repel the water. The simulation accurately predicted the average water velocities near the barrier, indicating its reliability for studying flow patterns around river bends with similar barriers. The results showed that the maximum shear stress on the barriers increased by 23.5 % for attractive structures and 17.6 % for repelling structures compared to vertical ones [10]. Karami *et al.* [11] worked on reduction of the erosion depth around a series of existing barriers in a river. They conducted experiments with an additional barrier placed upstream of the first one. They tested different designs by varying the size, length, angle, and spacing of the protective barriers under different water conditions. The results showed that a well-designed protective barrier can effectively reduce the maximum erosion depth around the main barriers, and specific design recommendations were provided based on the experiment's findings. [11]. Ning *et al.* [12] examined how the spacing between spur dikes affects the depth of erosion and flow characteristics. They found that the greatest erosion occurs near the first spur dike, and increasing spacing reduces its protective effect. The bed shear stress significantly influences the erosion process, as evidenced by correlation analysis. This factor also helps establish the optimal spacing for spur dikes, given that within the primary flow area, the maximum flow velocity is twice that of the incoming velocity. [12]. Esmaeli *et al.* [13] conducted a study to explore how modifying flow patterns through the use of spur dikes can help control erosion and protect river banks. The

study encompassed the creation of a laboratory meandering channel with the incorporation of five spur dikes, aiming to explore how erosion control is influenced by variations in both permeability and length [13]. Bora and Kalita [14] formulated a simulation-optimization framework aimed at identifying the most effective arrangement of groynes concerning their quantity, dimensions, and placements. This approach was designed to manage riverbank erosion successfully. The model minimizes construction costs while ensuring low flow speed in a specific zone to prevent erosion. The model utilizes the shallow water equations and a genetic algorithm for optimization, producing logical results and demonstrating its potential for real-world applications [14] lengths and positions for controlling bank erosion. The vulnerable bank is considered to be protected if a very small value of water flow speed is achieved on the near bank area. A linked simulation–optimization model is developed in this regard which minimizes the total construction cost of the groyne project. At the same time, a constraint in terms of low flow speed in a predefined zone is incorporated, which helps in bank erosion prevention. In the simulation model, the depth-averaged shallow water equations are solved using a finite difference scheme. The optimization problem is formulated in three different approaches to tackle different types of in situ field problems. Genetic algorithm (GA. Nayyer *et al.* [15] examined the flow characteristics around spur dikes of different shapes (I, L, T) arranged in series, both through experimental and numerical methods. It was determined that when employing a mix of (LTT) spur dikes, the most notable outcome was the reduction in velocity, shear stress, and turbulence intensity. This implies that the incorporation of different geometries in combination can effectively mitigate erosion and increase sedimentation amidst spur dikes [15]. Shamloo and Pirzadeh [16] investigated the behavior of subcritical flow around an indirect groyne by altering its installation angles. The objective was to analyze how these adjustments influence the extent of the separation zone that forms behind the groyne. By employing 3D simulations within the Fluent software, researchers observed a substantial influence of the angle of groyne installation on separation length. These findings exhibited a strong agreement with experimental data. The observed separation length was roughly 12 times that of a 0.3 m long impermeable

groyne. The angle that yielded optimal results was approximately 5 degrees, as indicated by Shamloo and Pirzadeh [16]. Zhang *et al*. [17] performed a series of experiments to explore the effects of single spur dikes, both permeable and impermeable, on beds prone to erosion. Their results indicated that the impermeable spur dike caused a maximum scour depth around it that was 50 % greater in comparison to the permeable spur dike [17]. Yang *et al*. [18] explored how the arrangement of permeable spur dikes within a river bend influences the highest water depth upstream. Their research indicated that placing the spur dikes at the midpoint of the bend, oriented at a 75° angle, specifically where the dike met the outer bank of the bend, caused formation of the greatest maximum depth of water [18].

The previous studies have dealt only with changes in river's morphology, pattern of mean velocity and resistance of flow [19-20]. With bridge pier and single impervious spur dike, the characteristics of flow as well as changes in morphology can be examined [21 In mountainous regions, the impervious spur dike has the advantage of non-formation of recirculation region around it but a slow flow field on the downstream side. Other models i.e., k –ε (epsilon model) and LES model were utilized to determine the maximum turbulent kinetic energy and scour hole at and around an impervious spur dike [9,17]. The reason of failure of impervious spur dike in alluvial rivers is scour hole of larger depth. It can be seen in Sangha Bridge Taunsa, Pakistan. All these models provide flow characteristics under specific conditions and do not provide information about recirculation zones behavior. In order to cope up with this, the present studies examine a model through we get complete information about the behavior of flow i.e., flow characteristics and recirculation zones behavior, by using different patches of dissimilar shapes at different positions within two impervious spur dikes.

2. METHODOLOGY

2.1 Equations for Numerical Simulation

The flow of water for the numerical simulation is assumed to be steady and incompressible. The Reynolds governing equations for numerical simulation are given below:

The flow of water for the numerical simulation is assumed to be steady and incompressible. The Reynolds governing equations for numerical simulation are given below:

The Continuity equation is:

$$\frac{\partial U_i}{\partial x_i} = 0$$

The Momentum equation is:

$$U_j \frac{\partial}{\partial x_j}(U_i) = \frac{v}{\rho}\frac{\partial}{\partial x_j}\left(\frac{\partial U_i}{\partial x_j} + \frac{\partial U_j}{\partial x_i}\right) - \frac{1}{\rho}\frac{\partial P}{\partial x_i} + (-\rho u_i u_j)$$

where $\frac{\partial R_{ij}}{\partial t}$ is the rate of change of Reynolds stresses, C_{ij} represents the convective transport, P_{ij} signifies the generation rate of Reynolds stresses, D_{ij} accounts for stress transport due to diffusion, ε_{ij} reflects the rate at which stresses dissipate, Π_{ij} characterizes the distribution of stresses resulting from interactions between turbulent pressure and strain and Ω_{ij} denotes the distribution of stresses due to rotational effects. where Ui and U$_j$ stands for the time-averaged velocity component along the x$_i$ and xy direction, v and ρ are the kinematic viscosity and density of the water respectively, P corresponds to pressure, and −ρu$_i$u$_j$ corresponds to the Reynolds stresses. The convective term is as follows:

$$C_{ij} = \frac{\partial(\rho U_k \overline{\acute{u}_i \acute{u}_j})}{\partial x_k}$$

The production term is:

$$P_{ij} = -(R_{im}\frac{\partial U_j}{\partial x_m} + R_{jm}\frac{\partial U_i}{\partial x_m})$$

The representation of the diffusion term is structured as follows:

$$D_{ij} = \frac{\partial}{\partial x_m}(\frac{v_t}{\sigma_k}\frac{\partial R_{ij}}{\partial x_m})$$

where, $v_t = C_\mu \frac{k_2}{\varepsilon}$, $C_\mu = 0.09$ and $\sigma_k = 1.0$.

The representation of the dissipation rate is structured as follows:

$$\varepsilon_{ij} = \frac{2}{3}\varepsilon \delta_{ij}$$

where ε symbolizes the rate of dissipation of turbulent kinetic energy and δ_{ij} corresponds to the Kronecker

delta. This delta δ_{ij} is equal to 1 when i equals j, and it is 0 when i is not equal to j.

$$\prod_{ij} = -C_1\frac{\varepsilon}{k}\left(R_{ij} - \frac{2}{3}kS_{ij}\right) - C_2(P_{ij} - \frac{2}{3}P\delta_{ij})$$

where C_1 and C_2 are 1.8 and 0.6, respectively. The turbulent kinetic energy k can be represented through the summation of three normal stresses:

$$k = \frac{1}{2}(\overline{\acute{u}_i{}^2} + \overline{\acute{u}_j{}^2} + \overline{\acute{u}_k{}^2})$$

The term of the rotation is given by:

$$\Omega_{ij} = -2\omega_k(\overline{\acute{u}_j\acute{u}_m}e_{ikm} + \overline{\acute{u}_i\acute{u}_m}e_{jkm})$$

The symbol ω_k represents the rotational vector, while e_{ijk} is known as the alternating symbol. This symbol e_{ijk} takes on a value of +1 when the indices i, j, and k follow a cyclic order and are distinct from each other. Conversely, when the indices i, j, and k are distinct but follow an anti-cyclic order, the alternating symbol e_{ijk} equals to -1. When any two indices among i, j, and k are identical, the alternating symbol takes on a value of 0.

2.2 Open Channel Specifications

To simulate the water flow for the analysis, the geometry of rectangular open channel is shown in Figure 1. The length of the open channel is 56 cm and the width is 96 cm. The maximum flow height is 7 cm. The spur dikes of specifications (4 x 24 x 7) cm were placed perpendicular to the mainstream as shown in Figure 1. The rectangular spur dikes are of impermeable nature which means that flow cannot pass through them. Within the field of impermeable spur dikes, vegetation patches (24 x 12 x 7) cm were placed at three positions bottom, middle and top. At each position, the arrangement and shapes were changed to investigate the displacement of recirculation region. The specifications for different shapes i.e., circular, prism, rectangular and different arrangements are shown in Figures 2-4.

The model was investigated such that each shape was placed at every position with both arrangements. So, for a total of 18 cases, the displacement of recirculation region was investigated through Reynold's stress turbulence model developed by
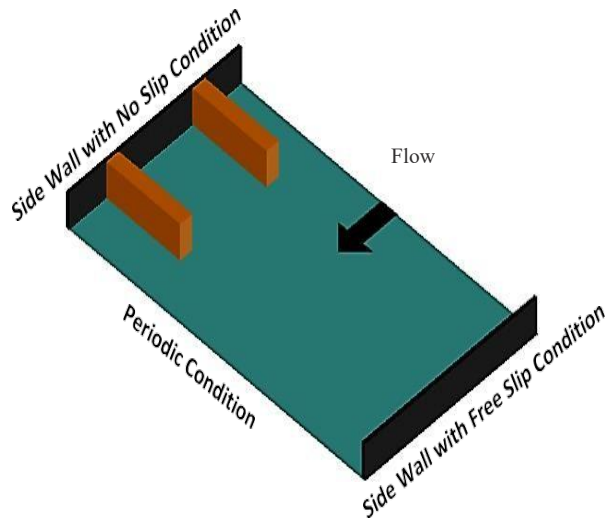
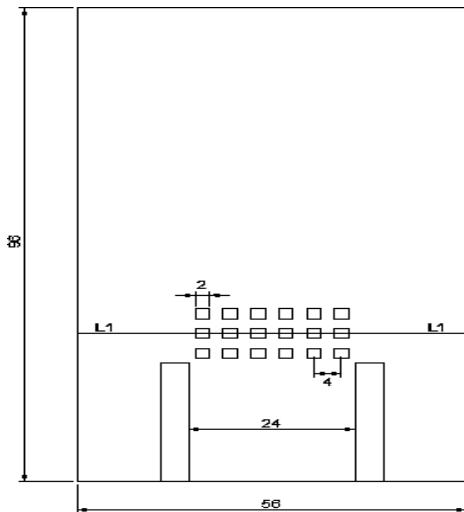**Fig. 1.** Arrangement for numerical simulation

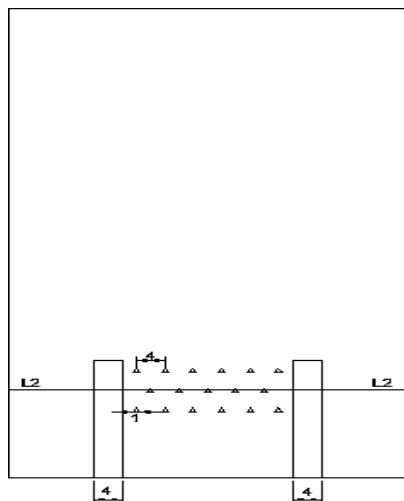**Fig. 2.** Rectangular top patch with linear arrangement

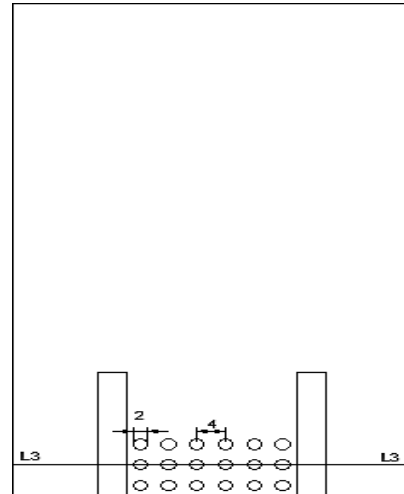**Fig. 3.** Prism middle patch with staggered arrangement

Fig. 4. Circular bottom patch with linear arrangement

three dimensional (3-D) numerical code FLUENT (ANSYS). At positions L1 (top), L2 (middle) and L3 (bottom) shown in Figures 2-4, the mean stream wise velocity profiles were drawn and at mid of flow depth i.e., 3.5 cm, a horizontal plane is made cut through the open channel for analyzing velocity contours and streamline flow.

3. RESULTS AND DISCUSSION

3.1 Mean Flow Characteristics

The mean stream wise velocity profiles for the total of 18 cases at the selected positions L1 (top), L2 (middle) and L3 (bottom) shown in Figures 2-4 are presented in Figure 5. From Figure 5, it can be clearly seen that at a certain position irrespective of the shape and arrangement of vegetation patch, the velocity profiles are somewhat similar. In other words, the shape and arrangement of the vegetation patch does not have significant influence on the velocity profile at a certain position. However, by changing the position of the vegetation patch, all three shapes and their respective arrangements show a change in the velocity profile. In Figure 5 (a-i) i.e., at the bottom position of the patch, all three shapes follow a similar velocity profile. The velocity at the upstream side is quite high than the downstream side, also within the field of impermeable spur dikes, the velocities are quite low. In Figure 5 (a-ii) for the staggered arrangement there is little variation in all three velocity profiles against each other with the prism shape showing the highest velocity profile. Also, within the field of

impermeable spur dikes, the fluctuations are more than with the linear arrangement with the prism shape showing more fluctuations than circular and rectangular shapes. In Figure 5 (b-i) i.e., at the middle position of the patch, the velocity profiles start at quite low values, then rapidly achieve peak velocities in comparison to the bottom position with the circular shape having the most peak velocity profile at both upstream and downstream side. In Figure 5 (b-ii), in case of staggered arrangement, all shapes follow the same trend for velocity profile similar to figure 5 (a-ii) but with the difference of having more peakedness added to the velocity profiles. In Figure 5 (c-i) i.e., at the top position, all three shapes show significant variation in velocity profiles at both upstream, downstream and within
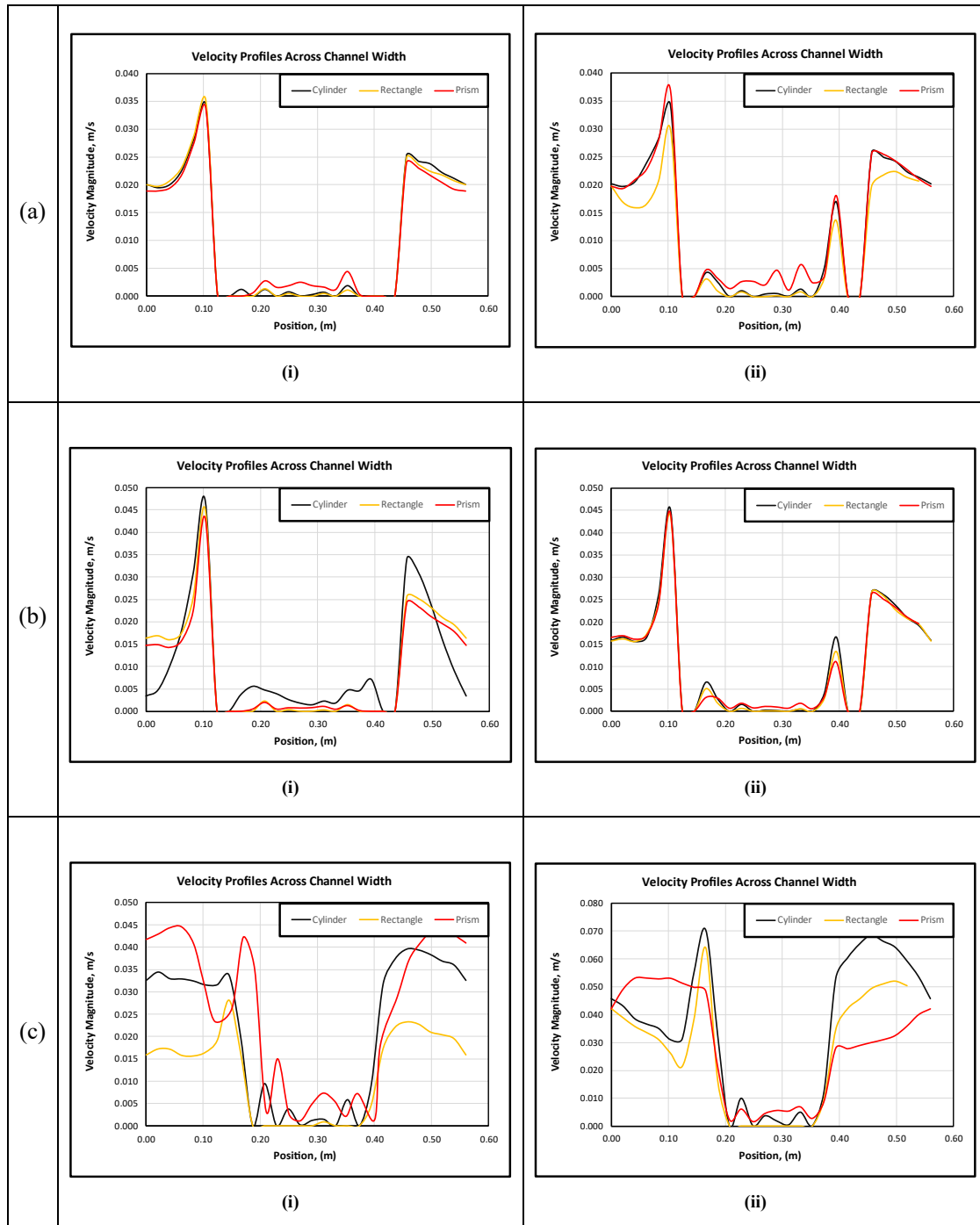

Fig. 5. Mean stream-wise velocity profiles i.e., across channel width 56 cm, (a) Patch position bottom (b) Patch position middle (c) Patch position top, (i) Linear arrangement (ii) Staggered arrangement

the field of impermeable spur dikes with the prism shape showing the most fluctuations throughout the stream flow and higher velocity than circular and rectangular shapes. In Figure 5 (c-ii), there is similar variation in the velocity profiles to that shown in 5 (c-i) but here, it can be concluded that out of all the 18 cases, this case where there is maximum velocity at both upstream and downstream side of the spur dikes and this highest velocity profile is shown by circular shape. Throughout all the cases the maximum velocity within the field of spur dike is of the order of 0.018 m/s which is quite low and can be the cause of recirculation regions formed within the field of impermeable spur dike.

3.2 Velocity Streamlines Characteristics

Next the recirculation regions are shown with the help of streamlines drawn on a horizontal plane at 3.5 cm of the maximum flow depth of 7 cm. At 3.5 cm that is the mid of flow depth (7 cm) a horizontal plane is cut through the entire open channel to visualize and observe the velocity streamlines around the spur dikes and vegetation patches as shown in Figure 6. The streamlines are shown for each shape at every position but only for linear arrangement as it is evident from the above discussion that the arrangement does not play significant role in altering the flow properties. The same streamlines can be assumed for the staggered arrangement. In Figure 6a, for the top patch position the recirculation region displaces as the shape of the vegetation patch is changed. In case of circular position, the recirculation region is somewhat in the middle of the field of impermeable spur dikes. As for rectangular shape, the recirculation is exactly at center and slightly above the middle of the field. While in the third case that is for prism
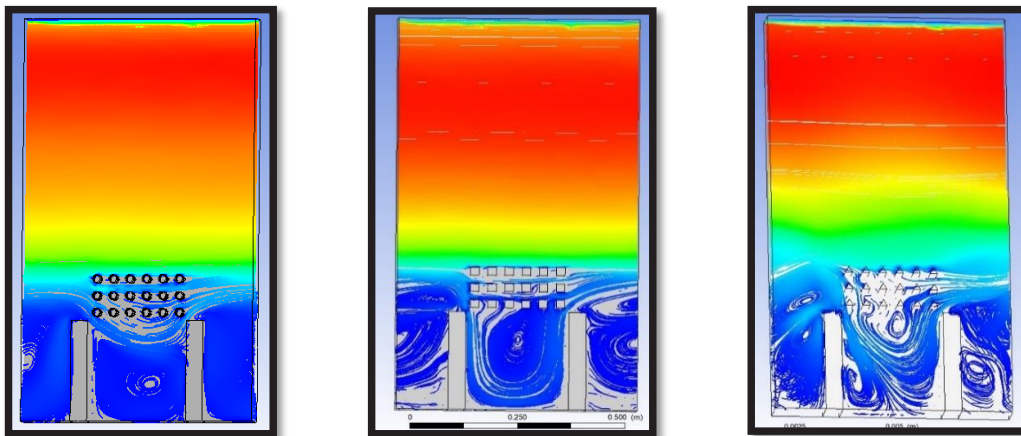

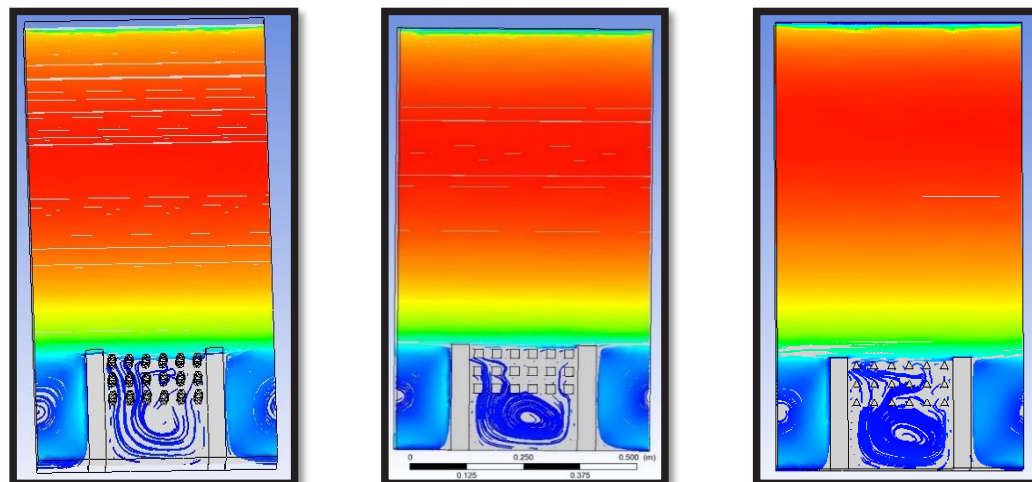**Fig. 6a.** Patch position top with linear arrangement, Left (Circular), Middle (Rectangular), Right (Prism)

Fig. 6b. Patch position middle with linear arrangement, Left (Circular), Middle (Rectangular), Right (Prism)
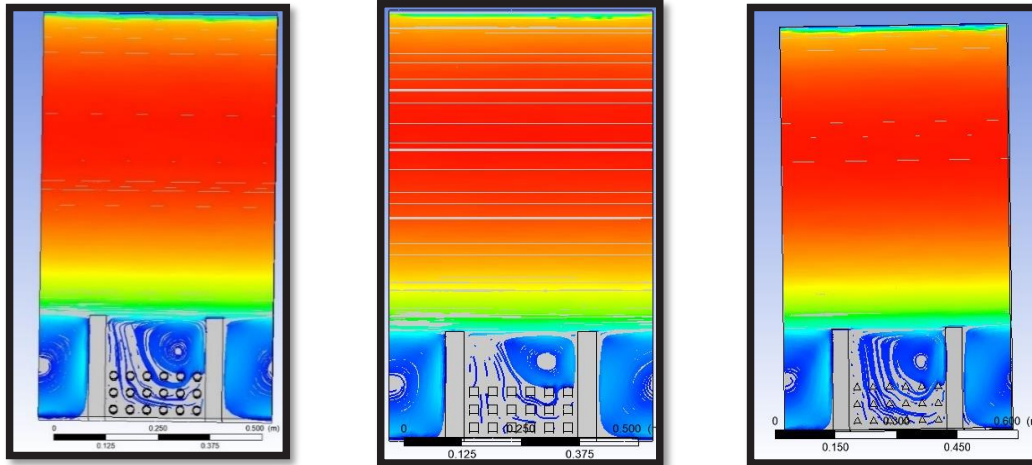
Fig. 6c. Patch position bottom with linear arrangement, Left (Circular), Middle (Rectangular), Right (Prism)

shape, there is a lot of turbulence, and more than one recirculation regions can be observed within the field of spur dikes. In Figure 6b, the position of recirculation region is same irrespective of the shape of vegetation patch for all three shapes the recirculation region is located in the middle of the field of impermeable spur dikes. However, the shape of recirculation region is not so prominent in case of the circular shape. In Figure 6c, for the bottom patch position, the location of recirculation region is identical for all three shapes i.e., top right corner of the field of two spur dikes. However, it can be noticed that for rectangular shape the shape of recirculation is bigger than for prism shape and that is in turn bigger than that for the circular shape.

4. CONCLUSION

The present investigation relates to study of the flow behavior in an open channel within impermeable spur dikes with vegetation patches of different shapes (circular, rectangular, prism) and arrangements (Linear and Staggered) laid in the field of the spur dikes at three different positions top, middle, and bottom. The main conclusions drawn out of this study are as following:

i. At a certain position irrespective of the shape and arrangement of vegetation patch, the velocity profiles are somewhat similar. In other words, the shape and arrangement of the vegetation patch does not have significant influence on the velocity profile at a certain position. By altering the vegetation patch position, the circular, rectangular, and prism shapes, along with

their respective arrangements, exhibit changes in velocity profiles.

ii. Throughout all the 18 cases discussed, the maximum velocity within the field of spur dike is of the order of 0.018 m/s due to the prism shape. This is quite low and can be the cause of recirculation zones within the region of spur dikes causing siltation.

iii. By changing the position of the vegetation patch, the location of recirculation region displaces within the field of impermeable spur dike. However, at a certain position, by changing the shapes and arrangement of vegetation patch, the location and shape of recirculation region is almost identical.

5. CONFLICT OF INTEREST

The authors declare no conflict of interest

6. REFERENCES

1   A.N. Giglou, J.A. Mccorquodale, and L. Solari. Numerical study on the effect of the spur dikes on sedimentation pattern. *Ain Shams Engineering Journal* 9(4): (2018).

2   M. Pandey, Z. Ahmad, and P.K. Sharma. Scour around impermeable spur dikes: a review. *ISH Journal of Hydraulic Engineering* 24(1): 1-20 (2018).

3   M. Koken. Coherent structures around isolated spur dikes at various approach flow angles. *Journal of Hydraulic Research* 49(6): 736-743 (2011).

4   M.R. Kafle. Numerical Simulation of Flow around a Spur Dike with Free Surface Flow in Fixed Flat Bed. *Journal of the Institue of Engineering* 9(1):

107-114 (2014).

5   H. Teraguchi, H. Nakagawa, K. Kawaike, Y. Baba, and H. Zhang. Effects of hydraulic structures on river morphological processes. *International Journal of Sediment Research* 26(3): 283-303 (2011).

6   N. Anjum, and N. Tanaka. Hydrodynamics of longitudinally discontinuous, vertically double layered and partially covered rigid vegetation patches in open channel flow. *Journal of River Research Applications* 36(1): 1-13 (2019).

7   S.-U. Choi, and H. Kang. Reynolds stress modeling of vegetated open-channel flows. *Journal of Hydrauic Research* 42(1): 3-11 (2004).

8   U. Ghani, N. Anjum, G.A. Pasha, and M. Ahmad. Numerical investigation of the flow characteristics through discontinuous and layered vegetation patches of finite width in an open channel. *Journal of Environmental Fluid Mechanics* 19(6): 1469-1495 (2019).

9   A. McCoy, G. Constantinescu, and L. Weber. Numerical Investigation of Flow Hydrodynamics in a Channel with a Series of Groynes. *Journal of Hydraulic Engineering* 134(2): 157-172 (2008).

10   M. Vaghefi, B. Faraji, M. Akbari, and A. Eghbalzadeh. Numerical investigation of flow pattern around a T-shaped spur dike in the vicinity of attractive and repelling protective structures. *Journal of the Brazilian Society of Mechanical Sciences and Engineering* 40(2): (2018).

11   H. Karami, A. Ardeshir, K. Behzadian, and M. Ghodsian. Protective spur dike for scour mitigation of existing spur dikes. *Journal of Hydraulic Research* 49(6): 809–813 (2011).

12   J. Ning, G. Li, and S. Li. Numerical simulation of the influence of spur dikes spacing on local scour and flow. *Journal of Applied Sciences* 9(11): 2306 (2019).

13   P. Esmaeli, S. Boudaghpour, M. Rostami, and M. Mirzaee. Experimental investigation of permeability and length of a series of spur dikes effects on the control of bank erosion in the meandering channel. *Ain Shams Engineering Journal* 13(4): 101701 (2022).

14   K. Bora, and H.M. Kalita. Determination of best groyne combination for mitigating bank erosion. *Journal of Hydroinformatics* 21(5): 875–892 (2019).

15   S. Nayyer, S. Farzin, H. Karami, and M. Rostami. A numerical and experimental investigation of the effects of combination of spur dikes in series on a flow field. *Journal of the Brazilian Society of Mechanical Sciences and Engineering* 41(6): 1-11 (2019).

16   H. Shamloo, and B. Pirzadeh. Numerical Simulation of the Angle of Groyne Installation on the Separation Zone Length Behind it. *Journal of River Engineering* 2(5): 2014.

17   H. Zhang, H. Nakagawa, K. Kawaike, and Y. baba. Experiment and simulation of turbulent flow in local scour around a spur dyke. *International Journal of Sediment Research* 24(1): 33-45 (2009).

18   J. Yang, J. Zhang, Q. Zhang, X. Teng, W. Chen, and X. Li. Experimental research on the maximum backwater height in front of a permeable spur dike in the bend of a spillway chute. *Journal of Water Supply* 19(6): 1841-1850 (2019).

19   M. Koken, and G. Constantinescu. An investigation of the dynamics of coherent structures in a turbulent channel flow with a vertical sidewall obstruction. *Journal of Physics of Fluids* 21: 085104 (2009).

20   S. Maeno, S. Ogawa, and Y. Uema. Local scour analysis around a spur dike during a surge pass. *Journal of Hydraulic Engineering* 48(2): 817-822 (2004).

21   N. Nagata, T. Hosoda, T. Nakato, and Y. Muramoto. Three-dimensional numerical model for flow and bed deformation around river hydraulic structures. *Journal of Hydraulic Engineering* 131(12): 1074-1087 (2005).